

The role of precipitation and irrigation on groundwater droughts in the Piemonte Plain, Italy

*Original*

The role of precipitation and irrigation on groundwater droughts in the Piemonte Plain, Italy / Ducco, E., Butera, I., Tamea, S.. - In: JOURNAL OF HYDROLOGY. REGIONAL STUDIES. - ISSN 2214-5818. - 65:(2026).  
[10.1016/j.ejrh.2026.103315]

*Availability:*

This version is available at: 11583/3009255 since: 2026-03-26T12:35:03Z

*Publisher:*

Elsevier

*Published*

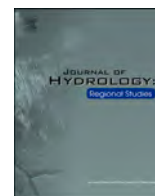
DOI:10.1016/j.ejrh.2026.103315

*Terms of use:*

This article is made available under terms and conditions as specified in the corresponding bibliographic description in the repository


*Publisher copyright*

(Article begins on next page)



## Article

# The role of precipitation and irrigation on groundwater droughts in the Piemonte Plain, Italy

Edoardo Ducco <sup>\*</sup> , Ilaria Butera, Stefania Tamea

Politecnico di Torino – Department of Environment, Land and Infrastructure Engineering, Corso Duca degli Abruzzi 24, Turin 10129, Italy

## ARTICLE INFO

## Keywords:

Groundwater drought  
 Meteorological drought  
 Irrigation  
 Aquifer recharge

## ABSTRACT

*Study region:* Piemonte Plain (upper Po plain), northwestern Italy.

*Study focus:* The relationship between meteorological and groundwater droughts of shallow aquifers is investigated in the Piemonte Plain, characterized by widespread irrigation, mainly supplied by Alpine-fed streamflow distributed through a complex irrigation network. Groundwater-level trends (2000–2023) were analyzed considering also seasonal behaviors. Anomalies in precipitation and groundwater levels were studied through the Standardized Precipitation Index (SPI) and Standardized Groundwater Index (SGI) across multiple time-windows and lags. A correlation-weighted lag was introduced to assess SPI–SGI response times during and outside the irrigation period. A conditional frequency analysis was carried out to study the propagation of meteorological drought into groundwater drought.

*New hydrological insights for the region:* The aquifer system exhibits a widespread decline over the 2000–2023 period. The analysis of the SPI–SGI correlations shows different results for the irrigation and non-irrigation periods. Irrigation weakens the relationship between precipitation and groundwater levels and the rice-cultivated area, mostly irrigated with flooding, shows the lowest SPI–SGI correlation values. The newly introduced weighted lag allows for a better characterization of groundwater response time to precipitation, overcoming the use of a single lag corresponding to maximum correlation. The propagation of meteorological drought into groundwater drought is disentangled during the irrigation period, mitigating SGI negative values in case of scarce precipitation.

## 1. Introduction

Among the extreme meteorological event and natural hazards, droughts are emerging as one of the most significant hydro-climatic challenges of the 21st Century (Sheffield and Wood, 2012; Trenberth et al., 2014). The term drought refers to a prolonged period of below-normal water availability, caused by persistent climatic conditions and human water demand (Tallaksen and Van Lanen, 2023; Wilhite et al., 2007).

Groundwater droughts, corresponding to a prolonged period of below-average groundwater levels, are caused by meteorological droughts (i.e. a lack or reduction in precipitation over a certain period (Mishra and Singh, 2010; Tate and Gustard, 2000), which reduce soil moisture and limit groundwater recharge, and by human activities such as abstractions and over-exploitations (Carlson et al., 2025; Mishra and Singh, 2010; Tallaksen and Van Lanen, 2023; Van Loon, 2015).

\* Corresponding author.

E-mail address: [edoardo.ducco@polito.it](mailto:edoardo.ducco@polito.it) (E. Ducco).

Previous studies show that groundwater droughts are less severe than meteorological droughts, exhibit a temporal delay, and have a longer duration (Bloomfield and Marchant, 2013; Kumar et al., 2016; Van Loon, 2015).

Future projections for the Mediterranean area, where the study area is located, indicate an increase in drought frequency and severity due to rising surface temperatures, particularly in spring and summer (Baronetti et al., 2022; Bloomfield and Marchant, 2013; Vicente-Serrano et al., 2010). An improvement towards sustainable regulation of groundwater usage will be crucial to manage future droughts periods (Elsaidy et al., 2025).

In this regard, the present work focuses on an approach to investigate the groundwater level dynamics and its connection to agricultural practices, considering the Piemonte region of Italy as case study. Piemonte region is a land rich of water, that in 2022 experienced a relevant drought event. This drought event highlighted the importance of groundwater resources and their vulnerability, and need to develop strategies to address and prevent future drought-related emergencies. An important point is the reduction of

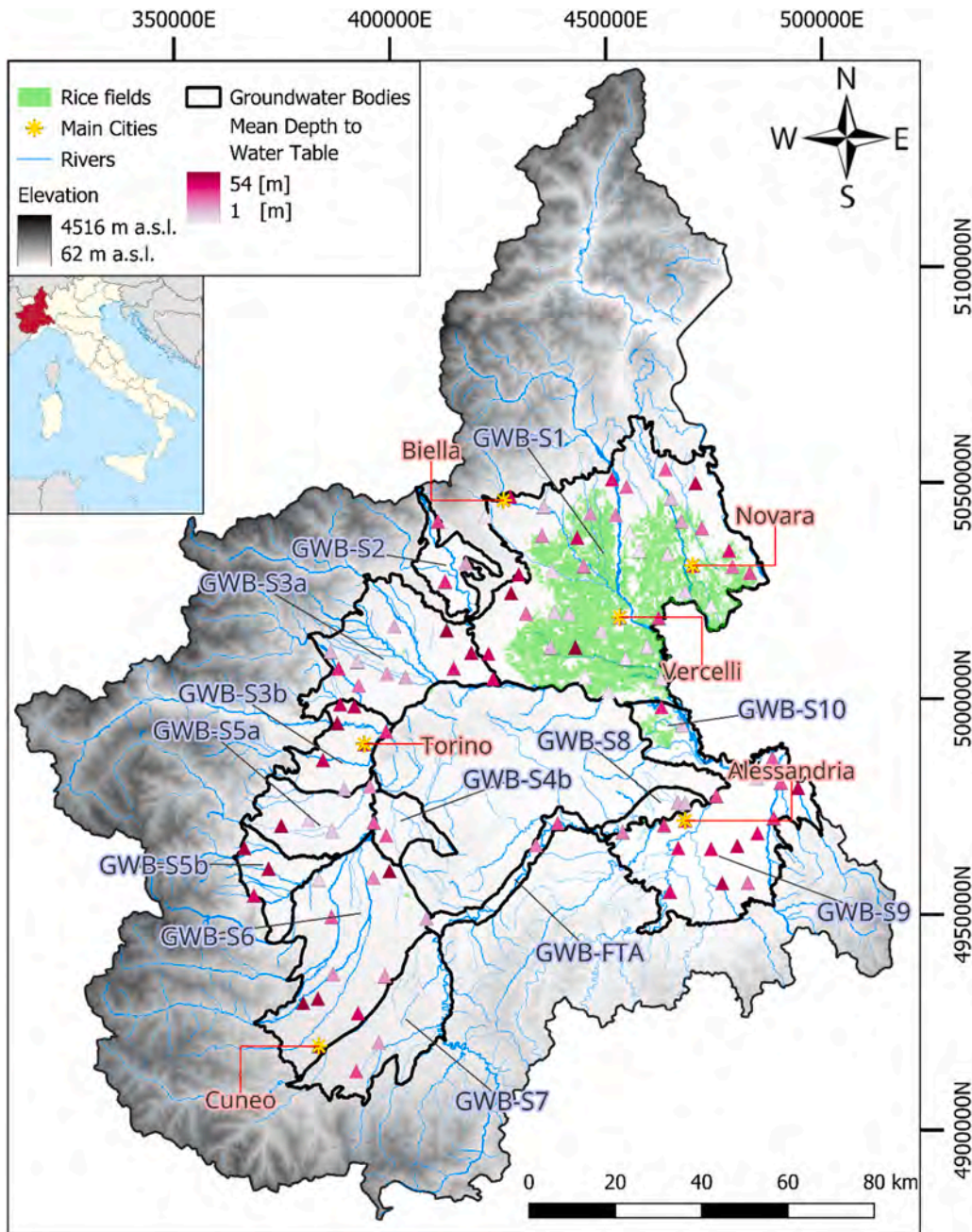


Fig. 1. Distribution of piezometers (displaying the mean depth to water table for the reference period) and groundwater bodies (GWBs) (black) in Piemonte. In green is represented the area related to rice fields.

water uses, for instance in irrigation practices. Understanding the impact of current irrigation practices on the groundwater levels before implementing changes, however, is necessary. Even if most irrigation water comes from surface waters in Piemonte region, shallow aquifers are of great importance. Irrigation practices in rice areas, for instance, rely on high groundwater levels that determine water springs with seasonal behavior, and in some periods of the year some canals and rivers are fed by the shallow aquifers.

Understanding the mechanisms of groundwater drought generation and propagation becomes crucial for developing effective solutions and strategies to enhance local and regional resilience to droughts in irrigated agricultural regions.

Different studies were performed in the past, focusing on the groundwater vulnerability of Piemonte region (Brussolo et al., 2022; Nistor, 2020), infiltration dynamics between the unconfined aquifers and the confined ones (Tamea and Butera, 2014), groundwater response to rainfall (Mancini et al., 2022) and to anthropogenic factors (Egidio et al., 2022; Lasagna et al., 2020). Lasagna et al. (2020) identified in the Piemonte Plain two groups of unconfined aquifer behavior: one linked to rainfall and one to land-use, such as urban and industrial areas, arable lands, rice fields and vineyards. Following this study, Mancini et al. (2022) study the trends of the groundwater level of the phreatic aquifer until 2017 and the connection with precipitation.

In comparison to previous studies, the present work uses a larger dataset of piezometric wells and investigates the influence of irrigation on groundwater drought propagation using the Standardized Groundwater Index (SGI) (Bloomfield and Marchant, 2013) and the Standardized Precipitation Index (SPI) introduced by McKee et al. (1993). This offers a novel contribution by quantifying the spatial and temporal variability of drought lag and attenuation. The correlation between SPI-SGI at different time windows and lags, and frequency of SGI events for certain SPI interval are investigated at each piezometer.

SGI is an indicator that allows for a characterization of groundwater level anomalies, enabling a detailed analysis of drought duration, intensity and response timing. SGI is based on the same methodology as SPI which characterizes precipitation anomalies.

Several studies have identified SGI-SPI correlation analysis as an useful tool for understanding the effect of precipitation on groundwater drought (Babre et al., 2022; Brakkee et al., 2021; Guo et al., 2021; Secci et al., 2021). A lag and an attenuation in the SGI as compared to SPI signal, due to the combined effect of soil hydraulic properties, withdrawals, land cover and proximity to rivers, was pointed out by several studies (Bloomfield et al., 2018, 2015; Van Loon, 2015).

## 2. Study area and data sources

### 2.1. Study area

This study considers the shallow aquifer of the Piemonte Plain, the westernmost extensions of the Po Plain, spanning 6890 km<sup>2</sup>. The Piemonte Plain is the most significant groundwater reservoir of the region due to its size, sedimentary characteristics, and recharge potential (Debernardi et al., 2008). The shallow unconfined aquifer lie within the alluvial deposits complex, with a thickness ranging from 20 to 50 m (Lasagna et al., 2020). Recharge areas for shallow groundwater are spread across the plain, primarily fed by rainfall infiltration and surface water contributions from rivers and canals (Lasagna et al., 2020). In the low plains, discharge areas are prominent, with the Po River serving as the primary regional axis for shallow groundwater outflow (Lasagna et al., 2020).

A 2017 field campaign measured water table depths in the shallow aquifers of the Piemonte Plain (Lasagna et al., 2020): in the northern plains, including the Torino and Cuneo plains (Fig. 1), and along main watercourses, water table depths were less than 5 m, in the eastern plains it varies on average in the range of 15–20 m, around 8–15 m in the South while the deepest water table depths, ranging from 35 to 40 m, occur in the western plains due to morphological terraces. The transit time in the unsaturated zone is generally less than a week, especially in the plain area. In all the morphologically highest areas of Biella, Cuneo, Novara and Vercelli, the transit time in the unsaturated zone is between 1 and 6 months (6 months in extremely small areas) (Regione Piemonte, 2021).

The Piemonte Plain hosts all major cities in the region, including Turin and its metropolitan area, with a population of approximately 2 million, highlighting its socioeconomic importance. Agriculture is present in Piemonte Plain: central and southern plains are used for the production of fruit, wine, cereals and legumes, while the northern plains of Novara and Vercelli are dedicated to the rice production. In Piemonte irrigation relies mainly on surface water diverted from the main rivers, distributed through a dense canal network managed by irrigation consortia under regional law. Rice fields in the Vercelli-Novara plains are supplied by large irrigation canals, where flooding remains the dominant irrigation technique. Maize and other crops are irrigated by surface, with limited adoption of sprinkler and drip systems due to costs and topographic constraints. Groundwater contributes significantly in hilly and marginal zones (Cuneo, Torino) where surface supply is scarce (Regione Piemonte, 2021). Artificial reservoirs and small basins complement river withdrawals, especially in areas with high variability of flows. In Piemonte is possible to identify two distinct periods: irrigation period from April to September and non-irrigation period from October to March. Regarding meteorological droughts, in the North of Italy for period 1971–2020 there is a trend towards dry conditions that is expected to continue in the following years with increased drought severity and duration (Baronetti et al., 2022).

### 2.2. Data

Precipitation data used in this study belong to the North Western Italy Optimal Interpolation (NWIOI) dataset, which contains daily precipitation values over a regular 24 × 20 cell grid, covering the area 6.5°E–9.5°E and 44.0°N–46.5°N with a resolution of 0.125° and a WGS84 (EPSG: 4326) projection. The available precipitation time series span from 1st December 1957–31 st March 2023. These data were obtained by the local environmental agency, ARPA, through the spatial interpolation of meteorological station point data (ARPA Piemonte, 2023a). Spatial data regarding groundwater bodies and the positions of the piezometers located in the shallow aquifer of the Piemonte Plain were sourced from ARPA Piemonte's "Portale delle Acque" (ARPA Piemonte, 2023b), using the WGS (EPSG: 4326)

projection. Daily groundwater level time series for the piezometers were provided by both ARPA Piemonte (ARPA Piemonte, 2023b) and Regione Piemonte (Regione Piemonte, 2018), comprising 125 piezometers from the automatic monitoring network of the shallow aquifer. Depending on the piezometer, the time series start between 2000 and 2002 and end in March 2023 and the precipitation data used for the analysis were limited to the same period.

Prior to conducting the analysis, a preprocessing phase was carried out to ensure homogeneous and uniform data. The groundwater level datasets included a “Flag” indicator, which takes a value of 1 when data has not been validated by the collector; approximately 1.53% of the total recorded data fell into this category and was excluded from the analysis avoiding potential errors. Next, daily values of groundwater levels and precipitation were aggregated into monthly time series. For the groundwater level series, the mean value of each month was computed, while for the precipitation series, the monthly summed value was calculated.

To ensure accurate calculations in subsequent analysis, a preprocessing workflow was applied to remove initial segments of time series with excessive non-valid or missing monthly values. Following this workflow, 106 piezometers with less than 40% missing data were selected for further analysis, of which 5 time series had no missing data.

To study the relationship between groundwater levels and precipitation, each piezometer time series was associated with the closest point on the precipitation data grid, ensuring both were within the same groundwater body. This association was carried out using the Voronoi polygons method applied to each GWB. The distribution of piezometers and GWBs in the Piemonte Plain is displayed in Fig. 1.

### 3. Methods

#### 3.1. Trend analysis with autocorrelation

In atmospheric and hydrologic research, the Mann-Kendall (MK) test, paired with the Sen’s slope estimation (Sen, 1968), is a widely used non-parametric method for trend analysis, based on ranking (Adombi et al., 2024; Collaud Coen et al., 2020). The computed statistics  $S$ , which counts the number of positive and negative changes between pairs of values, is normally distributed when the number of observations,  $N$ , exceeds 10. If  $S = 0$ , the null hypothesis is not rejected; while, if  $S > 0$  or  $S < 0$ , a monotonic trend is indicated. The test is performed by comparing the standardized test statistic  $Z = S/[\text{var}(S)]^{0.5}$  with the standard normal variate at the desired significance level. The Mann-Kendall test assumes statistical independence between observations, implying the absence of autocorrelation in the data. The adverse effect of data autocorrelation on Type 1 errors and biases in Sen’s slope estimation has been extensively studied (Hamed and Rao, 1998; Kulkarni and von Storch, 1995; Yue et al., 2002a), with findings showing that autocorrelation significantly increases Type-1 errors, whereas pre-whitening procedures can lead to an increase of Type-2 errors.

Given the high autocorrelation and non-stationary nature (long-term trend, seasonal variation) of monthly groundwater level time series, a pre-whitening step was necessary to reduce serial correlation in data. The Trend-Free Pre-Whitening Mann-Kendall with Yue’s modification (TFPW-Y), as proposed by Yue et al. (2002b), was employed. This approach was chosen over other pre-whitening methods due to its ability to preserve the test power in the case of strongly autocorrelated series, as in the case of groundwater levels (Adombi et al., 2024; Collaud Coen et al., 2020).

The TFPW-Y method follows these steps: (i) estimating the Sen’s slope on the original data; (ii) detrending the series to obtain a de-trended time series  $A^{detr}$ ; (iii) removing the lag-1 autocorrelation  $ak_1^{data}$  on  $A^{detr}$  to generate a de-trended pre-whitened time series  $A^{detr-prew}$ ; (iv) re-adding the original trend to generate the series  $S_t^{TFPW-Y}$  to which Mann-Kendall is applied. Trend analysis was carried out on monthly average groundwater levels and the Python package *pyMannkendall* developed by Hussain and Mahmud (2019) was used. In addition, the trend was quantified using the Sen’s slope (Sen, 1968), a non-parametric estimator of the slope of monotonic trend in a time series. Positive slopes indicate rising groundwater levels, while negative slopes reflect declining levels.

#### 3.2. Seasonal patterns of groundwater levels

Groundwater levels are strongly influenced by seasonal factors such as precipitation, evapotranspiration and agricultural practices (Bloomfield and Marchant, 2013; Green et al., 2011; Peters et al., 2003). To capture these variations in groundwater levels and intra-annual trends more effectively, the multi-annual time series per each month were considered separately to understand which periods contribute the most to long-term trends (Mirabbasi et al., 2020; Shanley et al., 2016). After pre-whitening the timeseries through the TFPW-Y method, a trend analysis was performed using the Mann-Kendall test (Gilbert, 1987; Mann, 1945). The Sen’s slope was then quantified to discriminate between rising and declining groundwater levels in the 12 months in each piezometer. To characterize the seasonal behavior levels, particularly the impact of irrigation, the results were classified into distinct patterns based on the presence of statistically significant trends among the 12 outcomes:

1. **Irrigation Pattern:** no significant trend is observed for the monthly time series outside the irrigation period, but at least 4 of the 6 months during the irrigation period exhibit statistically significant trends.
2. **Non-Irrigation Pattern:** no significant trend occurs for the monthly series during the irrigation period, but at least 4 of the 6 months outside the irrigation period show statistically significant trends.
3. **Yearly Pattern:** significant trends are observed in at least 9 months of the year, regardless of the irrigation period.
4. **No Pattern:** 3 months or less exhibit statistically significant trends.

### 3.3. Standardized precipitation index (SPI) and the standardized groundwater index (SGI)

The Standardized Precipitation Index (SPI), originally devised by [McKee et al. \(1993\)](#), measures standardized anomalies in precipitation and is used to quantify and compare dry or wet deviations. Precipitation input data can be aggregated on different time windows to delineate distinct types of drought ([Vincente-Serrano and López-Moreno, 2005](#)). A more detailed explanation of the SPI estimation procedure is given by [Edwards and McKee \(1997\)](#) and [Guttman \(1999\)](#).

In the present study, time windows of 1, 3, 6, 12 and 24 months were considered and for each time window, a parametric statistical distribution was computed for each location and month. To fit monthly precipitation data, the piece-wise Gamma probability distribution proposed by [Stagge et al. \(2015\)](#) was used to handle occasional zero precipitation values.

The standardized Groundwater Index (SGI) was developed by [Bloomfield and Marchant \(2013\)](#) to characterize groundwater droughts using groundwater level data, as input variable. SGI is a statistical indicator for groundwater drought based on the same concept of SPI, with values referring to standard normal distribution that measures deviations of groundwater levels from their median. Since common parametric distribution used for monthly precipitation (normal, log-normal and gamma) do not fit well monthly groundwater levels, previous studies have explored alternative distributions, such as the plotting position method and the kernel non-parametric distribution ([Bloomfield and Marchant, 2013](#); [Vidal et al., 2010](#)). In this work, Kernel Density Estimation (KDE) was used because the plotting position method was not considered suitable due to the limited length of the time series ([Secci et al., 2021](#)).

Monthly groundwater level data from each piezometer were used to fit the probability density function via KDE for each month and time window. The fitted probability density function was integrated to derive the cumulative density function, as shown in [Fig. 2](#), with groundwater levels on the x-axis and cumulative probability on the y-axis. Standardization of groundwater levels was achieved by performing an equiprobability transformation, converting the fitted distribution into a standard normal distribution. Positive SGI values indicate that groundwater levels are above the median of the period, representing surplus conditions, while negative values indicate deficit conditions.

In the subsequent sections, the terms  $SPI_i$  or  $SGI_i$  for a certain month denote the standardized indices for precipitation and groundwater, respectively, for an accumulation time  $i$  ending in the given month. SGI and SPI are typically divided into classes representing varying degrees of drought intensities. [Fig. 2](#) outlines the severity threshold established by [McKee et al. \(1993\)](#) and further adapted to groundwater by [Bloomfield and Marchant \(2013\)](#).

### 3.4. Correlation matrix

Correlation analysis between SPI and SGI has been widely used in previous studies to assess the linkage between precipitation variability and groundwater response ([Bloomfield and Marchant, 2013](#); [Guo et al., 2021](#); [Secci et al., 2021](#); [Uddameri et al., 2019](#)). The Pearson correlation coefficient ([Pearson, 1895](#)), defined as the ratio between the covariance and the product of the standard deviations of the two random sampled variables considered, measures the linear relationship between variables like SPI and SGI. Correlation of SPI and SGI was computed at different time windows ( $i = 1, 3, 6, 12, 24$  months). For each piezometer, results were organized in a square matrix where each row has a SGI time window value, and each column has a SPI time window value. The diagonal elements

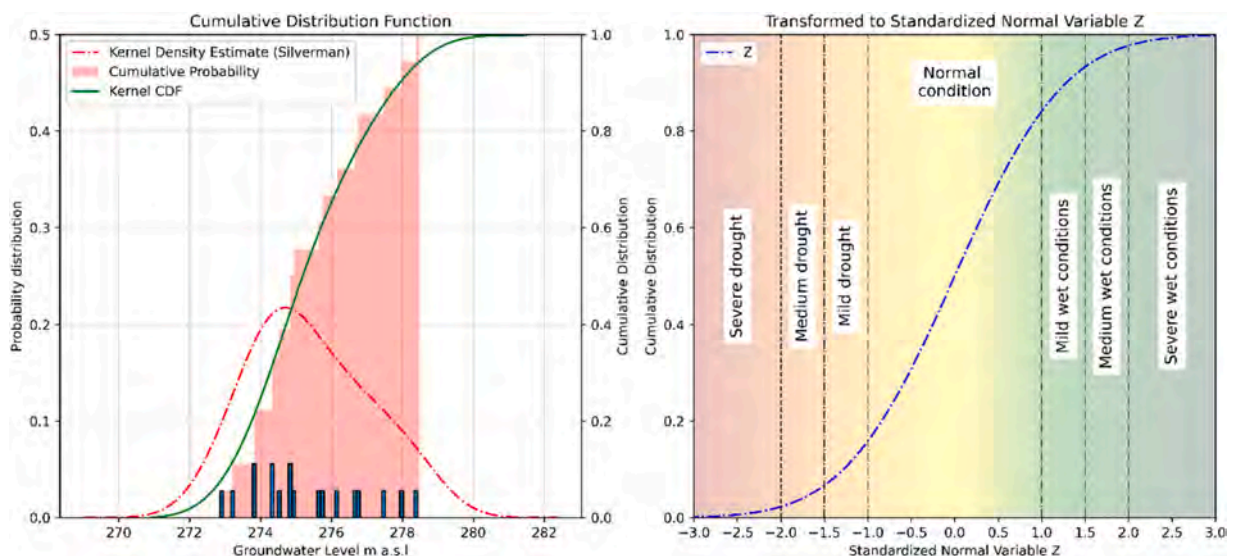


**Fig. 2.** Example of Standardized Groundwater Index construction for a piezometer located in Piemonte Region. The example refers to January SGI. The left panel shows the groundwater level data of January (in blue), the Kernel Density Estimate using Silverman method applied to groundwater level data (in red), the cumulative probability (red-filled area) and the Cumulative Distribution function using the Kernel (in green). The right panel shows the corresponding equiprobable standardized variable (SGI) and the ranges for drought classification according to [McKee et al. \(1993\)](#).

represent correlation between SPI and SGI at the same time windows. Values below the SW-NE diagonal represent the response of SGI to SPI across equal and longer time windows. Values above the diagonal, correlating precipitation with antecedent groundwater levels, were included just for completeness.

### 3.5. Lag analysis

A lag analysis was performed to study the possible relationship between SPI and SGI indices of different time windows, investigating the lagged-response of the aquifer to precipitation. This approach has been applied in previous studies to both precipitation-groundwater level data and on SPI-SGI indices (Babre et al., 2022; Bloomfield and Marchant, 2013; Brakkee et al., 2021; Secci et al., 2021). The lag analysis, applied to SPI and SGI indices, computed over a specific time windows, consist of shifting backwards in time the SPI index with a certain lag to explore the dependency of groundwater levels on antecedent precipitation. Preliminary analysis showed that many piezometers exhibit high correlation across multiple lags without a pronounced maximum. For each piezometer a new lag -  $lag_w$  - was defined as a weighted average of lags, with weights equal to the corresponding correlation coefficients. In order to emphasize the relevant delays, only lags showing correlation coefficients exceeding the mean correlation among all lags were considered. The new lag reads:

$$lag_w = \left( \frac{\sum_{i=1}^{Nm} L_i \rho_i}{\sum_{i=1}^{Nm} \rho_i} \right) \text{ if } \rho_i > \bar{\rho}, \quad \bar{\rho} = \left( \frac{1}{Nm} \right) \sum_{i=1}^{Nm} \rho_i \tag{1}$$

where  $L_i$  is the  $i^{th}$  lag,  $\rho_i$  is the corresponding correlation coefficient,  $\bar{\rho}$  is the mean correlation across all lags and  $Nm$  is the number of computed lags. This approach differs from previous studies that selected the lag corresponding to the maximum correlation (Babre et al., 2022; Bloomfield and Marchant, 2013; Guo et al., 2021) and gave unclear results in case of comparable adjacent maxima. In case of series exhibiting a periodic dynamics, which can lead to non-adjacent maxima, Eq. (1) should consider a time interval (in terms of  $Nm$ ) shorter than the time-series period.

### 3.6. Effect of irrigation on SPI-SGI correlation

The present study focuses on assessing the influence of irrigation on the relationship between SPI and SGI for the shallow aquifers of the area of interest. At this aim, for each piezometer SPI and SGI time series were divided into two subsets: one for the irrigation period (April-September) and another for the non-irrigation period (October-March). To perform the lag analysis the SPI<sub>*i*</sub>-SGI<sub>*i*</sub> ( $i = 1, 3, 6$ ) correlations were investigated constraining precipitation and groundwater levels inside the same sub-period. So doing, depending on the month considered for SGI<sub>*i*</sub> and the lag investigated, only precipitation time windows that are in the same irrigation/non-irrigation period than SGI<sub>*i*</sub> are listed, as function of the SPI<sub>*i*</sub> time windows and lag considered (Table 1).

### 3.7. Analysis of the drought propagation from meteorological to groundwater drought

Finally, a frequency-based evaluation of drought propagation, from meteorological to groundwater domains, was conducted to analyze the intensity of SGI events in response to specific SPI conditions. This evaluation can support the release of drought early warnings and can be useful to prepare probabilistic map concerning drought propagation (Seo and Lee, 2023).

The analysis considered for each piezometer all the monthly SGI<sub>*i*</sub> values and all the SPI<sub>*i*</sub> values for different time windows ( $i = 1, 3, 6$ ) to capture the varying temporal dependencies with SGI<sub>*i*</sub> considering separately irrigation and non-irrigation periods. This distinction enables a more detailed assessment of whether irrigation mitigates or exacerbates groundwater drought conditions under varying meteorological scenarios. With respect to the mentioned study (Seo and Lee, 2023), the improvement of the present work is the use of the lag into the computation of drought propagation frequencies to better capture the response of shallow aquifers levels to precipitations. To compute the drought propagation conditional relative frequencies, for each piezometer its characteristics  $lag_w$  of each sub-period (irrigation/non-irrigation) was used. For each SPI<sub>*i*</sub> and SGI<sub>*i*</sub> combination, the frequencies of occurrence of values in the following ranges were assessed: [(-3,-2); (-2,-1); (-1,0); (0,1); (1,2); (2,3)]. The conditional relative frequency of a SGI<sub>*i*</sub> value of ( $Y$ )

**Table 1**

Months considered for SGI<sub>*i*</sub> in each sub-period (irrigation and non-irrigation) according to SPI time windows and lags. Months are reported as numbers: January = 1, February = 2, March = 3, April = 4, May = 5, June = 6, July = 7, August = 8, September = 9, October = 10, November = 11, December = 12.

Lag	Irrigation Period			Non-Irrigation Period		
	SPI <sub>1</sub>	SPI <sub>3</sub>	SPI <sub>6</sub>	SPI <sub>1</sub>	SPI <sub>3</sub>	SPI <sub>6</sub>
0	4-5-6-7-8-9	6-7-8-9	9	10-11-12-1-2-3	12-1-2-3	3
1	5-6-7-8-9	7-8-9	-	11-12-1-2-3	1-2-3	-
2	6-7-8-9	8-9	-	12-1-2-3	2-3	-
3	7-8-9	9	-	1-2-3	3	-
4	8-9	-	-	2-3	-	-
5	9	-	-	3	-	-

falling within a specific range of values, given a SPI value ( $X$ ) falling within a specific range of values, was computed according to:

$$F(y_1 < Y \leq y_2 \mid x_1 < X \leq x_2) = \frac{N(y_1 < Y < y_2, \quad x_1 < X \leq x_2)}{N(x_1 < X \leq x_2)} \tag{2}$$

where  $N$  stands for number of cases in which the condition in parenthesis occurs, that is the numerator corresponds to the count of simultaneous occurrences of  $X(SPI_i)$  and  $Y(SGI_i)$  in their respective ranges, the denominator corresponds to the count of occurrences of  $X(SPI_i)$  in its range. For each combination of  $SGI_1$  and  $SPI_1$  ranges, the conditional relative frequencies obtained for all piezometers were subsequently averaged to obtain the final conditional relative frequency matrix, where SPI values are represented on the y-axis and SGI values on the x-axis.

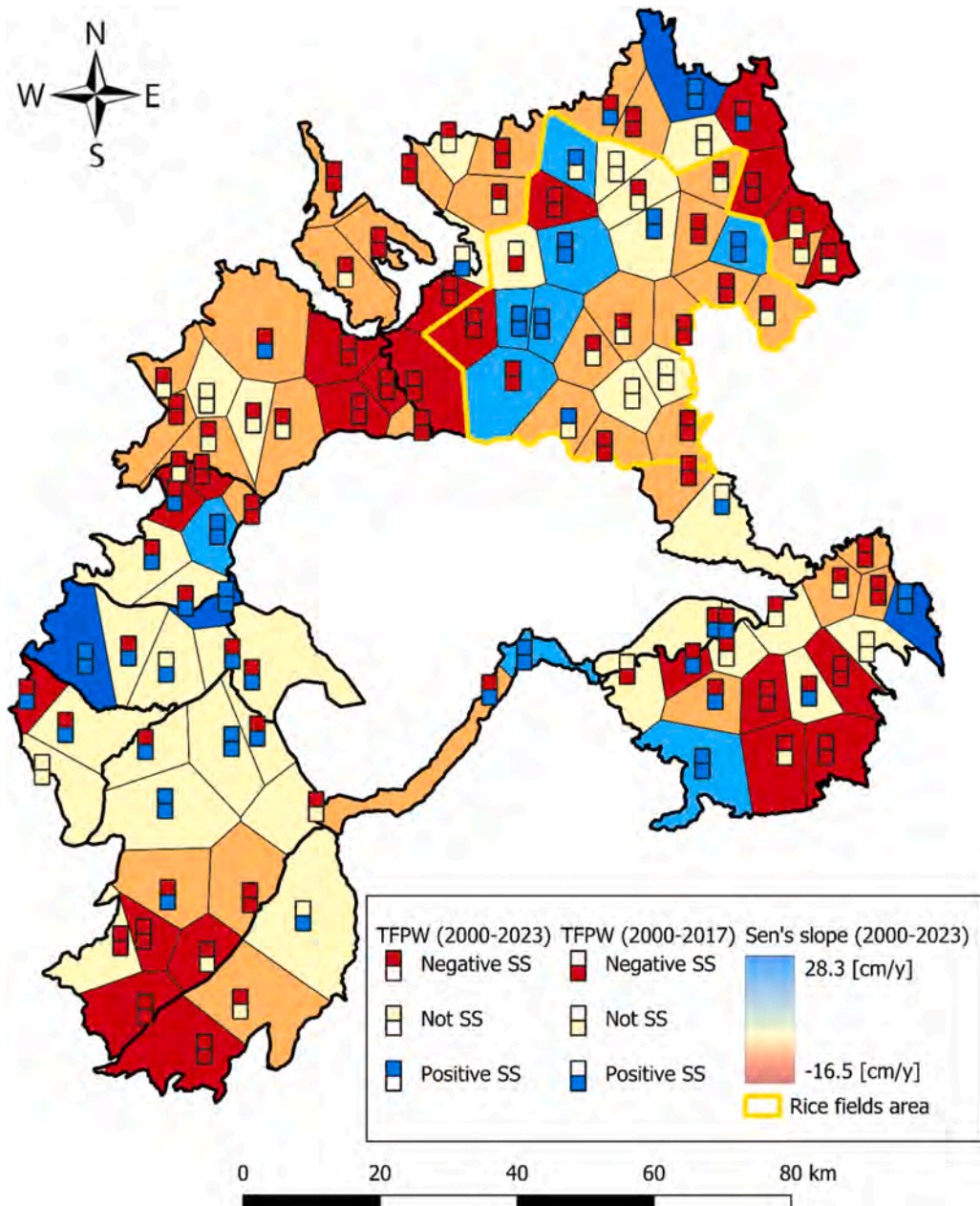


Fig. 3. Groundwater level trend in Piemonte Plain. The two boxes represent the statistically significance ( $\alpha = 0.05$ ) and the sign of the trend after TFPW pre-whitening method for period 2000–2023 (top) and period 2000–2017 (bottom). The Voronoi polygon of each piezometer is colored according to the slope of the Mann-Kendall test applied without pre-whitening.

## 4. Results

### 4.1. Trend analysis of groundwater level in Piemonte Plain (years: 2000–2023)

The analysis of monthly groundwater levels across 106 piezometers, employing time series over the period 2000–2023, reveals large autocorrelation. Autocorrelation is found to be greater than 0.7 and 0.9 in the 90% and 30% of the cases, respectively. Due to the presence of autocorrelation in the groundwater monthly level data, the TFPW-Y (Yue et al., 2002b) pre-whitening method was applied to all time series before the Mann-Kendall test. So doing, piezometers with statistically significant negative (77) and positive (16) trends were identified. The statistical significance and the sign of the trends are depicted in Fig. 3, showing for each piezometer the results with reference period 2000–2023 (top square). The trends do not exhibit a clear spatial pattern: strong negative trends are found in GWB-S6, GWB-S7, GWB-S3a and in GWB-S9, whereas the rice fields area in GWB-S1 exhibits a high heterogeneity with a generally stable trend prevailing across the piezometers.

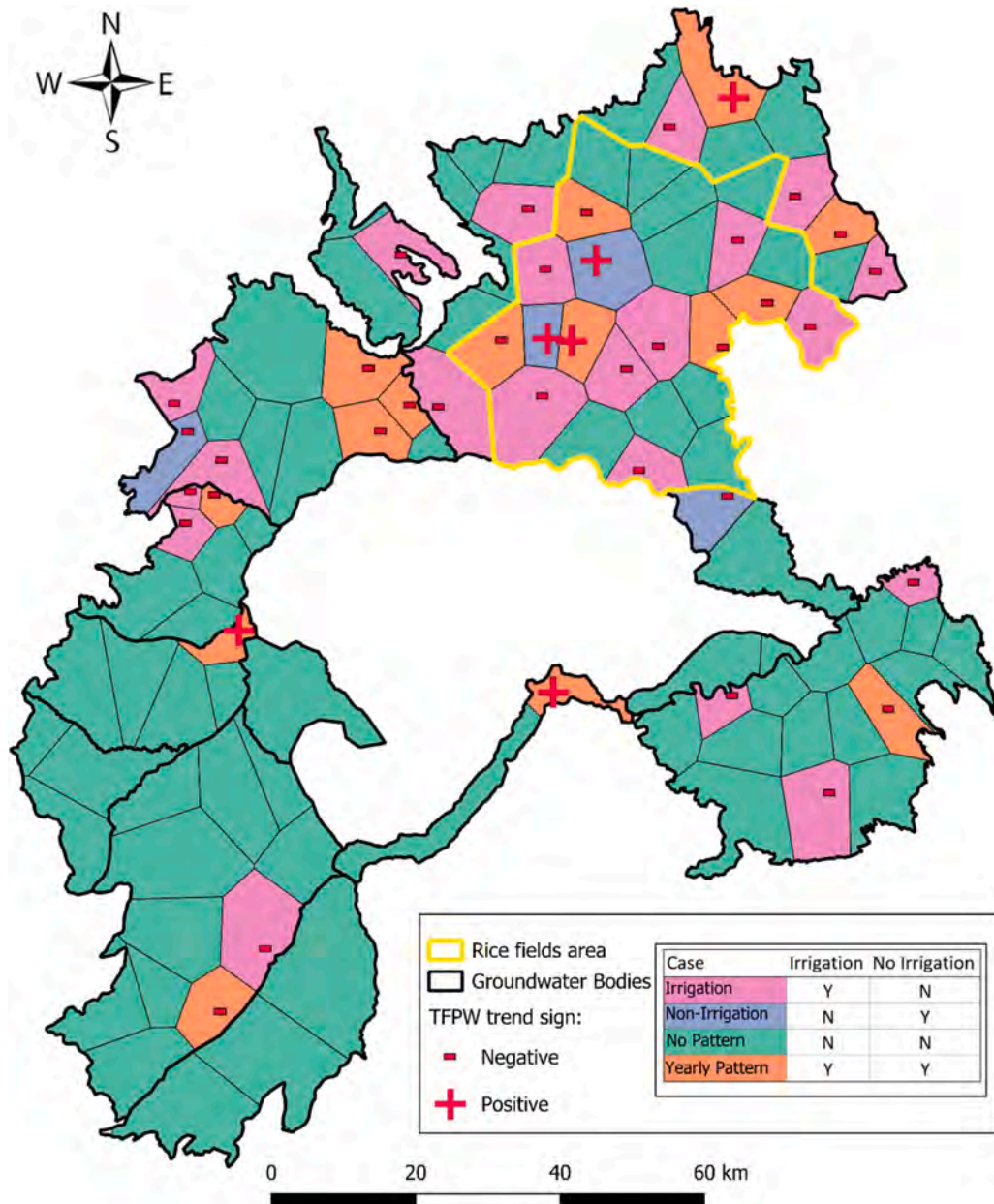


Fig. 4. Groundwater level trend at month-to-month scale over the period 2000–2023. The polygons are colored according to the pattern: Irrigation Pattern (pink), Non-Irrigation Pattern (indigo), Yearly Pattern (orange) and No Pattern (aqua green).

The TFPW-Y pre-whitening method was further compared to the Mann-Kendall test applied directly to the data 2000–2023 and displayed through the Voronoi polygons generated for each groundwater body based on the location of the piezometers. TFPW-Y detects more statistical significant trends than Mann-Kendall test with percentage increasing for increasing autocorrelation.

Trends obtained for years 2000–2023, and pre-processed by TFPW-Y method, are compared with those computed for years 2000–2017 obtained in prior studies (Mancini et al., 2022; Regione Piemonte, 2018) resulting in an increase of negative trends: out of the 36 negative trends of the period 2000–2017, 32 persist as statistically significant negative trends by 2023, among the 30 not statistically significant trends in period 200–2017, 23 evolve into statistically significant trends and of the 40 positive trends, 22 become negative. A consistent pattern of strong negative trends is evident for both periods, in the southwestern plains (GWB-S6 and GWB-S7), in the southeastern plains GWB-S9, and in GWB-S3a indicating a persistent decline in groundwater levels, highlighting long-term groundwater depletion.

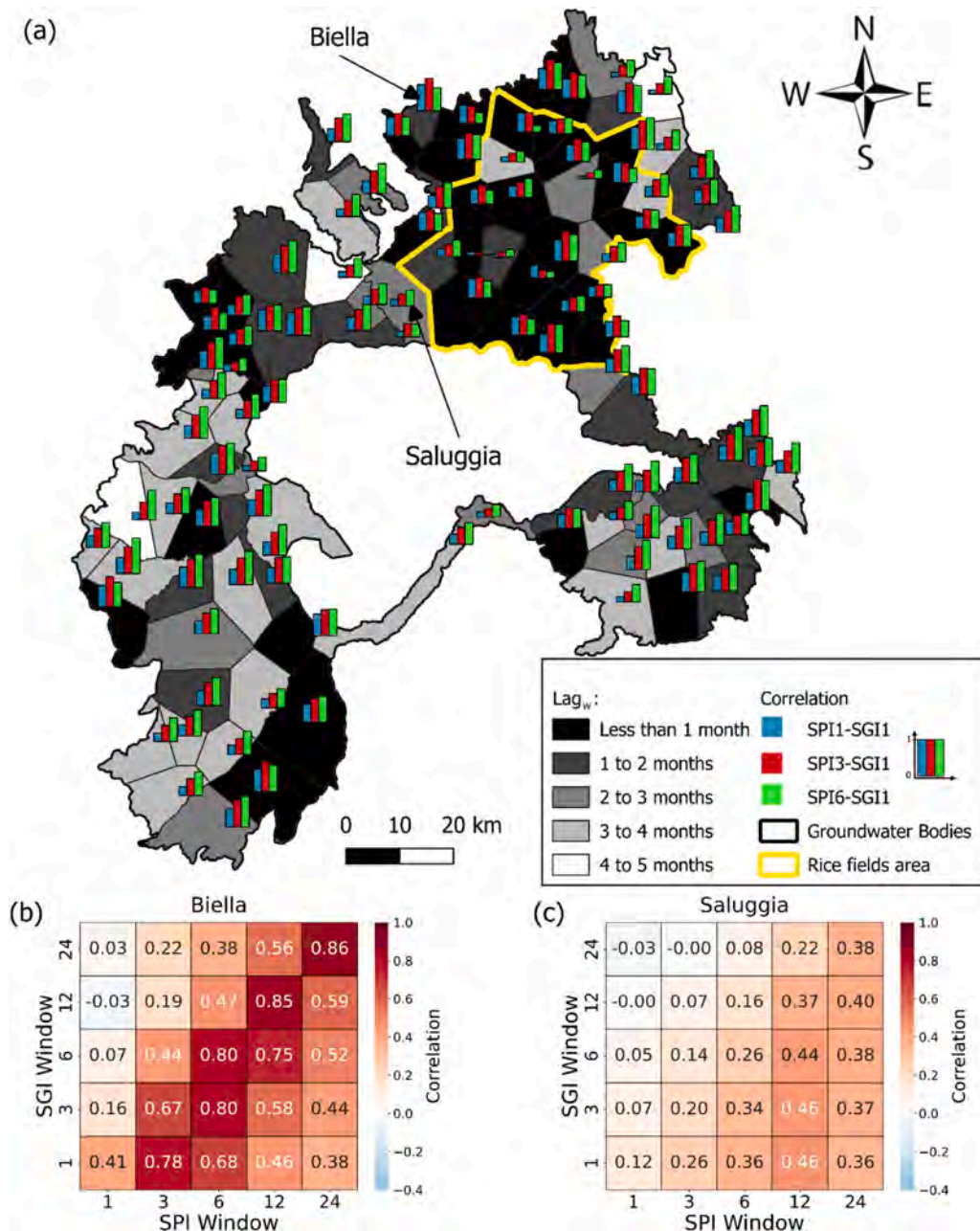


Fig. 5. Spatial variability of correlation between SPI<sub>1</sub> (i = 1, 3, 6) and SGI<sub>1</sub> at lag = 0 months. The blue column refers to SPI<sub>1</sub>, the red column to SPI<sub>3</sub> and the green column to SPI<sub>6</sub>. The Voronoi polygons are colored using a green to white color scale representing the lag<sub>w</sub> for the case SPI<sub>1</sub>-SGI<sub>1</sub>. Two correlation matrices are show as example.

#### 4.2. Monthly trends and seasonal patterns

The seasonality in the variation of groundwater levels was investigated conducting a trend analysis for each month and schematizing the patterns in relation to irrigation vs non-irrigation period. The analysis showed that none of the piezometers exhibit both positive and negative trends across the months (i.e. dual sign behavior), reflecting consistent directional trends in groundwater levels across all months, whose sign is shown in Fig. 4. Voronoi polygons of piezometers are colored according to the pattern (see also Section 3.2).

Polygons showing an Irrigation Pattern (significant trends in summer) are primarily located in the northern groundwater bodies, in areas typically associated with intensive agricultural activity and high irrigation demand partly related to rice cultivation. Among the 22 piezometers showing this behavior, 15 are located outside the rice field area (delimiting in yellow), while the remaining 7 are within it. All the 22 piezometers with the Irrigation Pattern exhibit negative trends, reflecting a year-over-year decline in seasonal groundwater levels. This behavior could be related to a decrease in the volume of water provided by irrigation, due for example by changes in cultivation/irrigation methods in rice production (Cocca et al., 2024), which impacts on the aquifer recharge rates. Piezometers exhibiting an Irrigation Pattern outside the rice fields are predominantly located close to mountain regions in the north-western portion of the Piemonte Plain. These piezometers show negative trends during the irrigation period, similar decreasing trends in groundwater levels due to reduced recharge from surface water have also been reported by Epting et al. (2021), who noted diminished recharge during the summer and autumn months in Alpine areas.

In contrast, areas showing a Non-Irrigation Pattern (trends are present out of irrigation periods) are fewer and sparsely distributed, with minimal clustering. Out of four cases, two piezometers located near rivers at the edges of the Piemonte Plain show slightly negative trends, which may suggest reduced infiltration from surface water. The other two piezometers are located within one kilometer of major irrigation canal (Canale Cavour), where winter water flows might have changed due to changed rice paddies flooding and new hydroelectric plants.

The Yearly Pattern (trend in more than 9 months) highlights mostly a groundwater depletion likely due to hydrological shortages or anthropogenic factors, such as industrial or urban water withdrawals demands. Among the 14 piezometers classified under this pattern, 12 are located within 1.5 km of surface water bodies, which strongly influences their trends, and 4 are situated at the terminal part of the irrigation network.

Lastly, No Pattern areas (trend in less than 3 months) are primarily located in the southern Piemonte Plains, mostly in areas with previously identified non-significant trends, referring to results in Section 4.1.

#### 4.3. Correlation and time dependence between SPI and SGI

The relationship between meteorological and groundwater droughts was investigated through the correlation analysis of the SPI and SGI indices. Fig. 6 shows the dependency of correlation  $SPI_i-SGI_1$  on the time-window employed for SPI without a lag. For lag = 0, the average correlation between  $SPI_1-SGI_1$  is low (0.32), whereas it increases for the case  $SPI_3-SGI_1$  (0.49) and for the case  $SPI_6-SGI_1$  (0.55). Results not shown here indicate that the  $SPI_i-SGI_1$  correlation does not increase for precipitation time window greater than 6 months. Two examples of correlation matrices are shown in Fig. 5 to show how SPI-SGI correlation can change in space for a case of high correlation (Biella) and a negligible correlation (Saluggia).

The comprehension of the behavior of  $SPI_i-SGI_1$  correlation is improved through the lag analysis. The correlation values of  $SPI_i-SGI_1$  ( $i = 1, 3, 6$ ) were studied for lag values varying from 0 to 5 months. As shown in Appendix A, the behavior of correlation for different lags is characteristic of each piezometer and highly depend on the time window. To avoid the effect of non-pronounced maximum values, the characteristic lag of each piezometer -  $lag_w$  - was computed using Eq. (1) for  $Nm = 5$  at most, coherent with the characteristic transit times through the unsaturated zone, and it came out that 1.89 months is the most frequent value delay in the response of  $SGI_1$  to  $SPI_1$ , 1.54 months to  $SPI_3$  and 1.34 months to  $SPI_6$ , as shown in Table 2.

For a comparison with the common method - lag at maximum correlation (Bloomfield and Marchant, 2013) - see the Supplementary material in Fig. A.9. The spatial distribution of  $lag_w$  does not display a significant spatial pattern as show in Fig. 5, for the  $SPI_1-SGI_1$  case. In general, the area with smaller  $lag_w$  are in the northern regions or close to mountains. Large  $lag_w$  corresponds to low correlation values for the three considered  $SPI_i$  time windows but not the opposite: low  $SPI_i-SGI_1$  correlation values can have small  $lag_w$ .

#### 4.4. SPI-SGI correlation and irrigation

To examine the different behaviors of the piezometric level during and outside the irrigation period. First, correlations between  $SPI_i$

**Table 2**  
Occurrences of  $lag_w$  for  $SPI_i-SGI_1$  ( $i = 1, 3, 6$ ).

Case	0-1	1-2	2-3	3-4	4-5
<b>SPI1-SGI1</b>	40	25	15	23	3
<b>SPI3-SGI1</b>	58	20	7	13	8
<b>SPI6-SGI1</b>	74	9	11	7	5

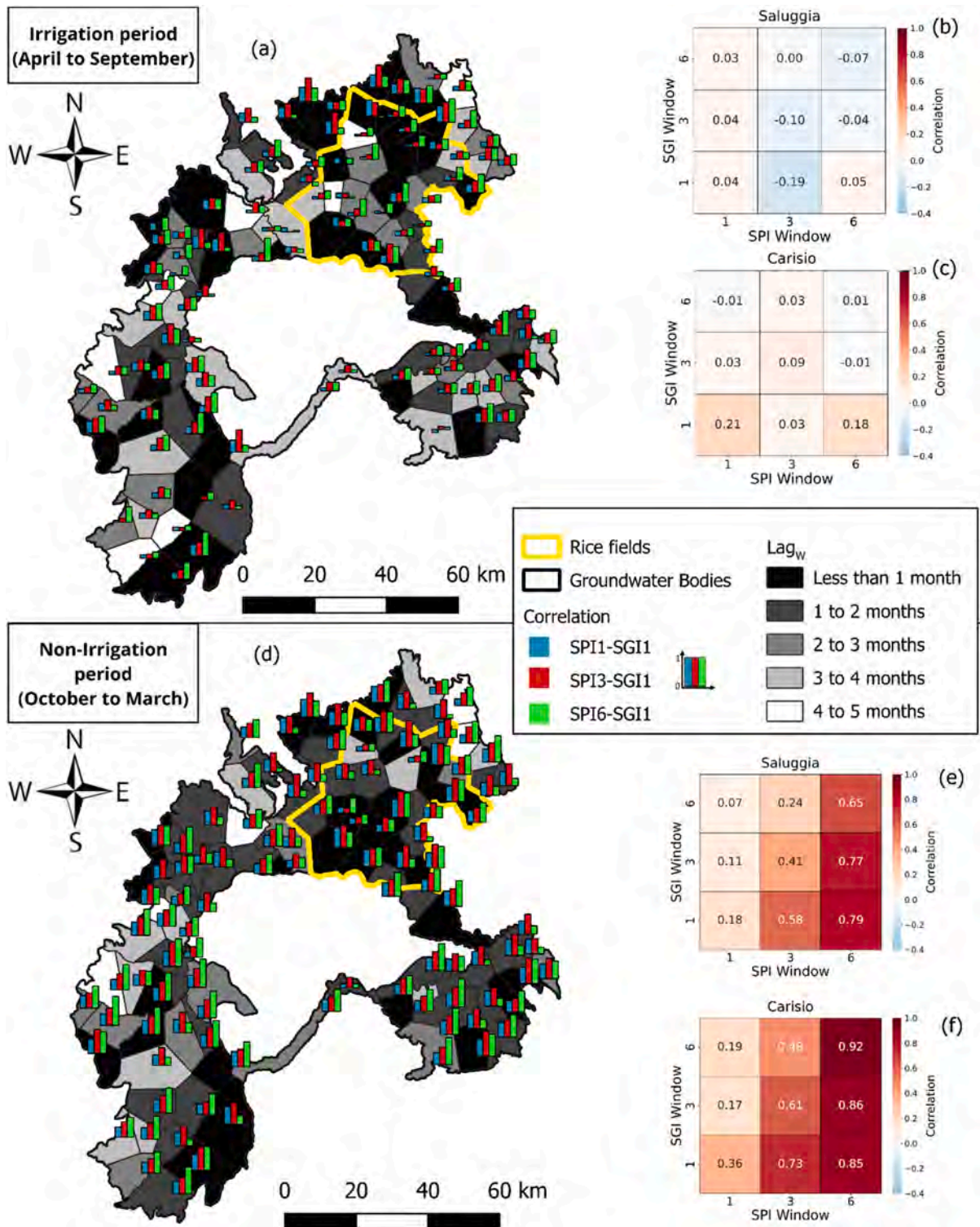


Fig. 6. Spatial representation of correlation and  $lag_w$  during (above) and outside (bottom) the irrigation period. For each piezometer histograms shows the correlation strengths of SPI<sub>1</sub>-SGI<sub>1</sub> (blue), SPI<sub>3</sub>-SGI<sub>1</sub> (red) and SPI<sub>6</sub>-SGI<sub>1</sub> (green) at lag = 0. The Voronoi polygons are colored according to the lag for SPI<sub>1</sub>-SGI<sub>1</sub> in irrigation and non-irrigation conditions, using a green to white color scale. At the bottom of the figure, two examples of correlation matrices with lag = 0 during and outside the irrigation period are reported.

( $i = 1, 3, 6$ ) and  $SGI_1$  with lag = 0 are evaluated for a fixed irrigation/non-irrigation period as explained in Section 3.6: for example,  $SPI_6$ - $SGI_1$  correlation values for the irrigation period can be computed only for September  $SGI_1$  and April to September  $SPI_6$  to stay within the irrigation period.

The histograms of Fig. 6 show the correlation strengths for the piezometers during (left) and outside (right) the irrigation period for lag = 0, while numerical data are presented in Table 3.

As it can be seen for all the  $SPI_i$ - $SGI_1$  cases, correlation is higher in the non-irrigation period. The effect of irrigation is, in fact, to interfere with the natural recharge from precipitation weakening the connection between precipitation and groundwater. In the  $SPI_1$ - $SGI_1$  case, the most notable correlation difference between irrigation and non-irrigation period is found in the southern groundwater bodies (GWB-S6, GWB-S7 and GWB-S9), with differences in the range 0.5–0.12, and in the rice field area with differences of 0.22 for  $SPI_3$ - $SGI_1$  and 0.50 for  $SPI_6$ - $SGI_1$ .

Rice flooding significantly disrupts the precipitation-groundwater relationship, lowering correlation values due to anthropogenic recharge overriding meteorological inputs. The correlation matrices in Fig. 6 are clear examples of how irrigation affects aquifer recharge. In fact, the response of groundwater levels to precipitation in the non-irrigation period is clear with higher and more significant  $SPI$ - $SGI$  correlation values.

Next, the analysis focused on the lagged response of the groundwater to precipitation in irrigation and non-irrigation conditions. The lag analysis was conducted for  $SPI_i$ - $SGI_1$  ( $i = 1, 3$ ) in the two sub-periods, constraining precipitation and groundwater levels in the same irrigation/non-irrigation period. As a consequence  $lag_w$  is limited to 5 and 3 for  $SPI_1$  and  $SPI_3$ , respectively. For completeness, in Appendix A, correlation values are displayed for lags until 12 months for both sub-periods. During the irrigation period, piezometers usually display low correlation values with small variations at different lags. During the non-irrigation period, instead, correlation is higher for lower lags (0, 1, 2 months mostly) and usually decreases as the lag increases.

The  $lag_w$  averaged over all the piezometers for the irrigation period is larger than in the non-irrigation period: 1.9 months and 1.7 respectively for the  $SPI_1$ - $SGI_1$  case and 1.5 and 0.9 for the  $SPI_3$ - $SGI_1$  case. The greater  $lag_w$  values, observed during the irrigation period, indicates that in this period  $SGI$  reacts more gradually to precipitation anomalies.

#### 4.5. Relative frequency evaluation of drought propagation from meteorological to groundwater droughts

A relative frequency evaluation of drought propagation from meteorological to groundwater drought was performed on the 106 piezometers located in Piemonte Plain, according to Section 3.7. The objective of the analysis was to retrieve which  $SPI$  values can trigger a  $SGI$  event in a certain range.

In Fig. 7, outcomes are displayed in two different forms. The heat maps in panel (a–f) are conditional relative frequency matrices, averaged on the 106 piezometers, for different combinations of  $SPI_i$  and  $SGI_1$  ranges under irrigation (top row) and non-irrigation (bottom row) conditions, considering  $SPI_1$ ,  $SPI_3$  and  $SPI_6$ . Each cell of the matrix shows the average conditional relative frequency among all the piezometers, of a  $SGI_1$  value within a certain range (on the columns) when  $SPI_i$  ( $i = 1, 3, 6$ ) is in a given range (on the rows). For a fixed  $SPI_i$  interval, that is a row of the panels, the relative frequency of the  $SGI_1$  intervals is shown so that the sum of the value of each row is 1. So doing, both the rows of a panel and the panels are comparable with each other.

In a situation of absence of irrigation drivers on the shallow aquifers higher relative frequencies are expected on the NW-SE diagonal where  $SPI$  and  $SGI$  values are in the same interval. This fact is evident in the non-irrigation period, especially for the  $SPI_6$ - $SGI_1$  case: strong negative  $SPI$  values are followed with higher conditional relative frequency by negative  $SGI$  values (panel e) and such negative  $SGI$  values are not reached in the irrigation period (panel c) where the effect of the irrigation on mitigating strong negative  $SPI$

**Table 3**

Correlation ranges, counts and mean values during irrigation and non-irrigation periods for  $SPI_i$ - $SGI_1$  ( $i = 1, 3, 6$ ) at lag = 0.

Case	Range	Irrigation		Non-irrigation	
		Count	Mean	Count	Mean
$SPI_1$ - $SGI_1$	< 0	1	-0.05	0	-
	[0,0.2]	60	0.13	6	0.17
	[0.2,0.4]	37	0.29	41	0.34
	[0.4,0.6]	8	0.46	57	0.47
	[0.6,0.8]	0	-	2	0.66
	> 0.8	0	-	0	-
$SPI_3$ - $SGI_1$	< 0	0	-	0	-
	[0,0.2]	25	0.13	0	-
	[0.2,0.4]	42	0.30	7	0.28
	[0.4,0.6]	26	0.46	37	0.51
	[0.6,0.8]	13	0.67	58	0.69
	> 0.8	0	-	4	0.83
$SPI_6$ - $SGI_1$	< 0	2	-0.10	0	-
	[0,0.2]	23	0.13	0	-
	[0.2,0.4]	42	0.31	7	0.33
	[0.4,0.6]	31	0.49	8	0.48
	[0.6,0.8]	8	0.69	55	0.70
	> 0.8	0	-	36	0.86

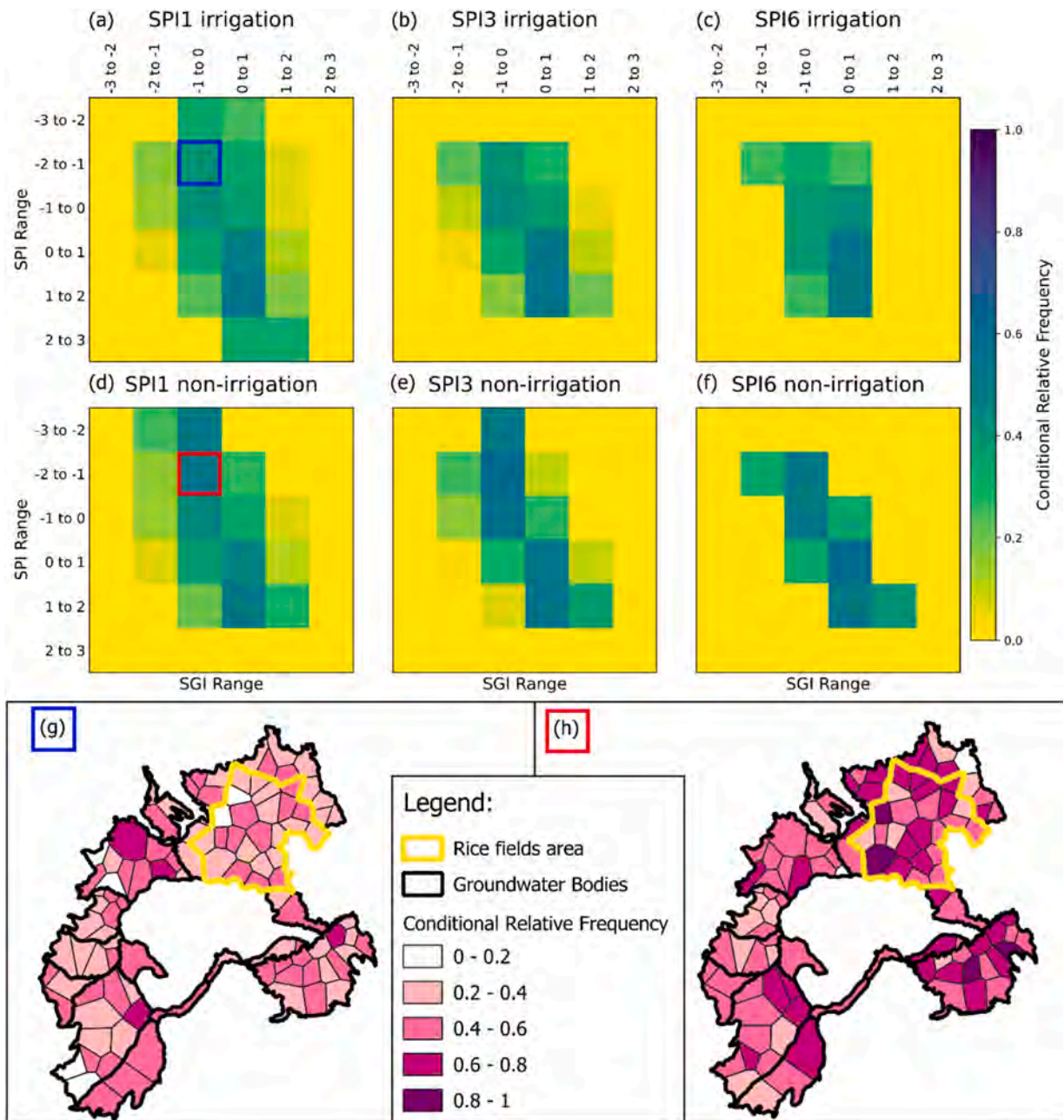


Fig. 7. Comparison of SPI1-SGI1 conditional relative frequency matrices under irrigation (a–c) and non-irrigation (d–f) conditions. Panels (g–h) displays the spatial distribution of conditional relative frequencies in irrigation (g) and non-irrigation (h) conditions.

events is evident. The conditional relative frequencies in the non-irrigation period (panel d–f) are more diagonalized compared for those of the irrigation period (panel a–c), showing the higher sensitivity of groundwater system to precipitation when irrigation is absent. In the irrigation case, instead, the conditional relative frequency of a negative SPI event to be followed by a mild negative SGI event, especially for  $i = 1$  and 3, as it can be seen in Fig. 7 (panels a–c). The maps of Fig. 7 show values averaged over the piezometers, and example of the spatial distribution of the conditional relative frequency is provided in Fig. 7 (panels g–h) for the case:  $-2 < SPI_1 < -1$  (mild to moderate meteorological drought) paired with  $-1 < SGI_1 < 0$  (normal to mild groundwater drought). It can be seen that the frequency of mild groundwater drought in the rice area during the irrigation is lower than in other parts.

### 5. Discussion

The current trend analysis indicates a general depletion of shallow aquifers, with a larger share of areas showing statistically

significant negative trends compared with previous studies (Mancini et al., 2022). This is partially motivated by the advanced trend detection method (TFPW-Y) applied to cope with the strong autocorrelation in groundwater level time series (Hamed and Rao, 1998; Yue et al., 2002b). The use of TFPW-Y is appropriate for monthly groundwater levels because it mitigates the lag-1 dependence while preserving trend signal. Beside the methodological improvement, the increase in negative trend cases compared with 2000–2017 (Mancini et al., 2022) suggests that the depletion has strengthened in the most recent years, consistently with an overall deepening in several groundwater bodies.

The trend's spatial heterogeneity suggests a superposition of multiple drivers, including water withdrawals, river-aquifer interaction, surface irrigation, managed recharge, local hydrogeology. The understanding of groundwater level dynamics and the connection with aquifer recharge and irrigation practices is thus a necessary step in the comprehension of the role played by such drivers.

The monthly trend classification highlighted that trends are not uniformly distributed through the year. Negative significant trends in the April-to-September occur mainly in northern groundwater bodies and indicate long-term changes in the irrigation period groundwater regime. Given the sensitivity of groundwater levels to irrigation practices in the study area (Egidio et al., 2022) (irrigation recharge, canal seepage, abstraction), negative trends in the shallow aquifer in rice-cultivated areas are consistent with changes in cultivation and irrigation method (Cocca et al., 2024), which impact on the aquifer recharges rates. Unfortunately, data on irrigation practices (traditional flooding vs dry seeding) are not available and it is difficult to perform an in-depth analysis on the effect of these factors.

The correlation analysis shows that SPI3-SGI1 and SPI6-SGI1 correlations are higher than SPI1-SGI1 and that correlation do not further increase for SPI windows longer than 6 months. This behavior is consistent with groundwater integrating precipitation anomalies over multiple months, as commonly reported in the literature (Bloomfield and Marchant, 2013; Guo et al., 2021; Secci et al., 2021; Uddameri et al., 2019). The analysis carried out separately for the irrigation and the non-irrigation period clearly shows that the effect of irrigation (both through pumped water and through water withdrawn from rivers) is to interfere with the groundwater recharge from precipitation and to lower the SPI-SGI correlation. Overall in the Piemonte region, the influence of irrigation reduces such correlation and delays the response of groundwater system to precipitation, with a stronger effect in rice cultivated areas, where irrigation recharge can override meteorological inputs and groundwater variability cannot be explained by precipitation anomalies alone.

To clarify the role of irrigation on groundwater levels the frequency analysis was determinant. Conditional relative frequency matrices show a more diagonal structure in the non-irrigated period, indicating that meteorological drought classes translate more consistently into concordant groundwater drought classes when irrigation is not active. During irrigation, the matrices are less diagonal and strong negative SPI values are followed less frequently by strong negative SGI outcomes, dampening drought propagation, despite the existing withdrawals for irrigation from shallow aquifers. Through the canal leakages and the existing surface irrigation system, irrigation acts as a buffer against short-term climatic variability, delaying hydrological responses by smoothing input anomalies and prolonging the infiltration/percolation process that contribute to groundwater recharge. Spatial examples confirm that this smoothing is not uniform and is strongest in rice systems, highlighting the importance of stratifying drought diagnostic by irrigation practices.

These results indicate that groundwater drought behavior in Piemonte is strongly shaped by irrigation, which reduces SPI-SGI correlation, increases apparent lag-response dispersion and attenuates drought propagation during irrigation period. Therefore, drought monitoring frameworks based solely on climatic indices risk to not characterize well groundwater vulnerability.

It is worth noting that a limitation of this study lies in the lack of data on irrigation volumes and calendars, both from surface water and pumped water. This type of information would allow for water balance assessments and a deeper analysis of the heterogeneity of irrigation impacts over the area. Although the 2000–2023 piezometric record supports robust monthly analysis, longer time series would better resolve decadal variability, but such records are not available across the Piemonte Plain monitoring network.

## 6. Conclusions

The present study investigates the interplay between meteorological and groundwater droughts in the Piemonte region (Italy) through trend analysis and standardized drought indices. The results show that current irrigation practices, acting as a source of aquifer recharge in the region, mask the effect of precipitation anomalies in smoothing meteorological droughts.

In light of these findings, the effects of changing irrigation strategies to reduce water consumptions (i.e., shift from flooding to dry seeding of rice, reduction of irrigation network leakages, crop change) must be carefully assessed, not only in terms of water use efficiency but also in terms of their impacts on aquifer recharge and drought recovery in the long period. To this goal, in the evaluation of new irrigation practices, it would be important to develop decision support systems based on the simulation of irrigation networks and their connection with field irrigation and shallow aquifers, providing a quantitative support for irrigation management and planning.

This study showed the results of Piemonte region, but the methodology applied is a novel, transferable methodology to quantify groundwater-climate linkages under anthropogenic influence and supporting a more accurate groundwater drought diagnosis in increasingly managed and stressed hydrological systems.

Among the future development of this research, the role of temperature on irrigation requirements and a detailed analysis of most recent groundwater drought can be considered. Some preliminary analysis, not show for sake of brevity, show that the rice area were less affected by prolonged drought conditions both in term of groundwater drought severity and speed of recovery from a drought.

Finally based on the results of this work, practical recommendations are as follows: (i) the planning of irrigation changes (e.g. dry

seeding, leakage reduction, crop changes) should be evaluated using indicators that account for groundwater recharge and its drought recovery; (ii) drought monitoring and early-warning drought systems in irrigated areas should integrate meteorological and groundwater indicators and consider irrigation and non-irrigation periods; (iii) water managers are recommended to develop an accurate monitoring system of irrigation flows, pumping volumes and irrigation calendars and (iv) are invited to share these information with the scientific community to enable the development of decision support systems and digital twins for irrigation that can improve the quantitative knowledge of the irrigation-groundwater system and enable an accurate and holistic assessment of water management choices and their effects on surface and groundwater resources.

### CRediT authorship contribution statement

**Ilaria Butera:** Writing – review & editing, Writing – original draft, Supervision, Conceptualization. **Stefania Tamea:** Writing – review & editing, Supervision, Funding acquisition, Conceptualization. **Edoardo Ducco:** Writing – review & editing, Writing – original draft, Software, Data curation, Conceptualization.

### Declaration of Competing Interest

The authors declare that they have no known competing financial interests or personal relationships that could have appeared to influence the work reported in this paper.

### Acknowledgements

The authors acknowledge funding from the European Union's Horizon Europe programme under Grant Agreement No. 101112876, MountResilience.

### Appendix A. Supporting information

Supplementary data associated with this article can be found in the online version at [doi:10.1016/j.ejrh.2026.103315](https://doi.org/10.1016/j.ejrh.2026.103315).

### Data availability

The data are provided by Regione Piemonte and ARPA

### References

- Adombi, A.V.D.P., Chesnaux, R., Boucher, M.-A., 2024. Toward a methodology to explore historical groundwater level trends and their origin: the case of Quebec, Canada. *Environ. Earth Sci.* 83, 183.
- ARPA Piemonte, 2023. Portale delle acque - acque sotterranee.
- ARPA Piemonte, 2023. Dataset su griglia NWIOI.
- Babre, A., Kalvans, A., Avotniece, Z., Retike, I., Bikse, J., Jemeljanova, K.P.M., Zelenkevics, A., Delina, A., 2022. The use of predefined drought indices for the assessment of groundwater drought episodes in the Baltic States over the period 1989–2018. In: *Journal of Hydrology: Regional Studies*. Elsevier. <https://doi.org/10.1016/j.ejrh.2022.101049>.
- Baronetti, A., Dubreuil, V., Provenzale, A., Fratianni, S., 2022. Future droughts in northern Italy: high-resolution projections using EURO-CORDEX and MED-CORDEX ensembles. *Clim. Change* 172, 22.
- Bloomfield, J.P., Marchant, B.P., 2013. Analysis of groundwater drought building on the standardised precipitation index approach. In: *Hydrology and Earth System Sciences*, 17. European Geosciences Union, pp. 4769–4787. <https://doi.org/10.5194/hess-17-4769-2013>.
- Bloomfield, J.P., Marchant, B.P., Bricker, S.H., Morgan, R.B., 2015. Regional analysis of groundwater droughts using hydrograph classification. In: *Hydrology and Earth System Sciences*, 19. European Geoscience Union, pp. 4327–4344. <https://doi.org/10.5194/hess-19-4327-2015>.
- Bloomfield, J.P., Marchant, B.P., McKenzie, A.A., 2018. Increased incidence, duration and intensity of groundwater drought associated with anthropogenic warming. *Hydrol. Earth Syst. Sci. Discuss.* 2018, 1–23. <https://doi.org/10.5194/hess-2018-244>.
- Brakkee, E., van Huijgevoort, M., Bartholomeus, R.P., 2021. Spatiotemporal development of the 2018–2019 groundwater drought in the Netherlands: a data-based approach. *Hydrol. Earth Syst. Sci. Discuss.* 2021, 1–26. <https://doi.org/10.5194/hess-2021-64>.
- Brussolo, E., Palazzi, E., von Hardenberg, J., Masetti, G., Vivaldo, G., Previati, M., Canone, D., Gisolo, D., Bevilacqua, I., Provenzale, A., et al., 2022. Aquifer recharge in the Piedmont Alpine zone: historical trends and future scenarios. *Hydrol. Earth Syst. Sci.* 26, 407–427. <https://doi.org/10.5194/hess-26-407-2022>.
- Carlson, G., Massari, C., Rotiroli, M., Bonomi, T., Preziosi, E., Wilder, A., Whitaker, D., Grotto, M., 2025. Intensive irrigation buffers groundwater declines in key European breadbasket. *Nat. Water* 110.
- Cocca, D., Lasagna, M., Debernardi, L., Destefanis, E., De Luca, D.A., 2024. Hydrogeochemistry of the shallow aquifer in the western Po Plain (Piedmont, Italy): spatial and temporal variability. *J. Maps* 20, 2329164.
- Collaud Coen, M., Andrews, E., Bigi, A., Martucci, G., Romanens, G., Vogt, F.P., Vuilleumier, L., 2020. Effects of the prewhitening method, the time granularity, and the time segmentation on the Mann–Kendall trend detection and the associated Sen's slope. *Atmos. Meas. Tech.* 13, 6945–6964.
- Debernardi, L., De Luca, D.A., Lasagna, M., 2008. Correlation between nitrate concentration in groundwater and parameters affecting aquifer intrinsic vulnerability. *Environ. Geol.* 55, 539–558.
- Edwards, D.C., McKee, T.B., et al., 1997. Characteristics of 20th century drought in the United States at multiple time scales. *Colo. State Univ. Libr.*
- Egidio, E., Lasagna, M., Mancini, S., De Luca, D., et al., 2022. Climate impact assessment to the groundwater levels based on long time-series analysis in a paddy field area (Piedmont region, NW Italy): preliminary results. *ACQUE Sotter.* 11, 21–29.
- Elsaidy, A., Yimer, E.A., Mogheir, Y., Huysmans, M., Villani, L., Van Griensven, A., 2025. Groundwater drought and anthropogenic amplifiers: a review of assessment and response strategies in arid and semi-arid areas. *Sci. Total Environ.* 978, 179406.

- Epting, J., Michel, A., Affolter, A., Huggenberger, P., 2021. Climate change effects on groundwater recharge and temperatures in Swiss alluvial aquifers. *J. Hydrol.* **X**, 11, 100071.
- Gilbert, R.O., 1987. *Statistical Methods for Environmental Pollution Monitoring*. John Wiley & Sons.
- Green, T.R., Taniguchi, M., Kooi, H., Gurdak, J.J., Allen, D.M., Hiscock, K.M., Treidel, H., Aureli, A., 2011. Beneath the surface of global change: Impacts of climate change on groundwater. *J. Hydrol.* **405**, 532–560. <https://doi.org/10.1016/j.jhydrol.2011.05.002>.
- Guo, M., Yue, W., Wang, T., Zheng, N., Wu, L., 2021. Assessing the use of standardized groundwater index for quantifying groundwater drought over the conterminous US. In: *Journal of Hydrology*, 598. Elsevier. <https://doi.org/10.1016/j.jhydrol.2021.126227>.
- Guttman, N.B., 1999. Accepting the standardized precipitation index: a calculation algorithm 1. *JAWRA J. Am. Water Resour. Assoc.* **35**, 311–322. <https://doi.org/10.1111/j.1752-1688.1999.tb03592.x>.
- Hamed, K.H., Rao, A.R., 1998. A modified Mann-Kendall trend test for autocorrelated data. *J. Hydrol.* **204**, 182–196.
- Hussain, M., Mahmud, I., 2019. pyMannKendall: a python package for non parametric Mann Kendall family of trend tests. *J. Open Source Softw.* **4**, 1556.
- Kulkarni, A., von Storch, H., 1995. Monte Carlo experiments on the effect of serial correlation on the Mann-Kendall test of trend. *Meteorol. Z.* **4**, 82–85.
- Kumar, R., Musuza, J.L., Van Loon, A.F., Teuling, A.J., Barthel, R., Ten Broek, J., Mai, J., Samaniego, L., Attinger, S., 2016. Multiscale evaluation of the standardized precipitation index as a groundwater drought indicator. *Hydrol. Earth Syst. Sci.* **20**, 1117–1131. <https://doi.org/10.5194/hess-20-1117-2016>.
- Lasagna, M., Mancini, S., De Luca, D.A., 2020. Groundwater hydrodynamic behaviours based on water table levels to identify natural and anthropic controlling factors in the Piedmont Plain (Italy). *Sci. Total Environ.* **716**, 137051. <https://doi.org/10.1016/j.scitotenv.2020.137051>.
- Mancini, S., Egidio, E., De Luca, D.A., Lasagna, M., 2022. Application and comparison of different statistical methods for the analysis of groundwater levels over time: response to rainfall and resource evolution in the Piedmont Plain (NW Italy). *Sci. Total Environ.* **846**, 157479. <https://doi.org/10.1016/j.scitotenv.2022.157479>.
- Mann, H.B., 1945. Nonparametric tests against trend. *Econ. J. Econ. Soc.* **245**–259. <https://doi.org/10.2307/1907187>.
- McKee, T.B., Doesken, N.J., Kleist, J., et al., 1993. The relationship of drought frequency and duration to time scales. In: *Proceedings of the 8th Conference on Applied Climatology*. Boston, pp. 179–183.
- Mirabbasi, R., Ahmadi, F., Jhajharia, D., 2020. Comparison of parametric and non-parametric methods for trend identification in groundwater levels in Sirjan plain aquifer, Iran. *Hydrol. Res.* **51**, 1455–1477.
- Mishra, A.K., Singh, V.P., 2010. A review of drought concepts. *J. Hydrol.* **391**, 202–216.
- Nistor, M.-M., 2020. Groundwater vulnerability in the Piedmont region under climate change. *Atmosphere* **11**, 779. <https://doi.org/10.3390/atmos11080779>.
- Pearson, K., 1895. Notes on regression and inheritance in the case of two parents. In: *Proceedings of the Royal Society of London*, **58**. The Royal Society, pp. 240–242. <https://doi.org/10.1098/rsp1.1895.0041>.
- Peters, E., Torfs, P.J.J.F., Lanen, H.A.V., Bier, G., 2003. Propagation of drought through groundwater – a new approach using linear reservoir theory. In: *Hydrological Processes*, **17**. Wiley. <https://doi.org/10.1002/hyp.1274>.
- Piemonte, R., 2021. *Idrogeologia - Tempo di arrivo in falda (TOT)*. Regione Piemonte, 2018. Piano di tutela delle acque - Allegato3B. Regione Piemonte.
- Secci, D., Tanda, M.G., D’Oria, M., Todaro, V., Fagandini, C., 2021. Impacts of climate change on groundwater droughts by means of standardized indices and regional climate models. In: *Journal of Hydrology*, **603**. Elsevier. <https://doi.org/10.1016/j.jhydrol.2021.127154>.
- Sen, P.K., 1968. Estimates of the regression coefficient based on Kendall’s tau. *J. Am. Stat. Assoc.* **63** (324), 1379–1389. <https://doi.org/10.1080/01621459.1968.10480934>.
- Seo, J.Y., Lee, S.-I., 2023. Probabilistic evaluation of drought propagation using satellite data and deep learning model: from precipitation to soil moisture and groundwater. *IEEE J. Sel. Top. Appl. Earth Obs. Remote Sens.* **16**, 6048–6061.
- Shanley, J.B., Chalmers, A.T., Mack, T.J., Smith, T.E., Harte, P.T., 2016. Groundwater level trends and drivers in two northern New England glacial aquifers. *JAWRA J. Am. Water Resour. Assoc.* **52**, 1012–1030.
- Sheffield, J., Wood, E.F., 2012. *Drought: Past Problems and Future Scenarios*. Routledge.
- Stagge, J.H., Tallaksen, L.M., Gudmundsson, L., Loon, A.F.V., 2015. Candidate distribution for climatological drought indices (SPI and SPEI). In: *International Journal of Climatology*, **35**. Royal Meteorological Society, pp. 4027–4040. <https://doi.org/10.1002/joc.4267>.
- Tallaksen, L.M., Van Lanen, H.A., 2023. *Hydrological Drought: Processes and Estimation Methods for Streamflow and Groundwater*. Elsevier.
- Tamea, S., Butera, I., 2014. Stochastic description of infiltration between aquifers. *J. Hydrol.* **510**, 541–550.
- Tate, E., Gustard, A., 2000. Drought definition: a hydrological perspective. In: *Drought and Drought Mitigation in Europe*. Springer, pp. 23–48.
- Trenberth, K.E., Dai, A., Jones, G. van der S., P.D., Barichivich, J., Briffa, K.R., Sheffield, J., 2014. Global warming and changes in drought. In: *Nature Climate Change* **4**. Nature, pp. 17–22. <https://doi.org/10.1038/nclimate2067>.
- Uddameri, V., Singaraju, S., Hernandez, E., 2019. Is standardized precipitation index (SPI) a useful indicator to forecast groundwater droughts?—Insights from a Karst aquifer. *JAWRA J. Am. Water Resour. Assoc.* **55**, 70–88.
- Van Loon, A.F.V., 2015. Hydrological drought explained. In: *Wires Water*, **2**. Wiley Interdisciplinary reviews, pp. 359–392. <https://doi.org/10.1002/wat2.1085>.
- Vicente-Serrano, S.M., Begueria, S., López-Moreno, J.I., 2010. A multiscalar drought index sensitive to global warming: the standardized precipitation evapotranspiration index. In: *Journal of Climate* **N.23**. American Meteorological Society, pp. 1696–1718. <https://doi.org/10.1175/2009JCLI2909.1>.
- Vidal, J.P., Martin, E., Franchistéguy, L., Habets, F., Soubeyroux, J.M., Blanchard, M., Baillon, M., 2010. Multilevel and Multiscale drought reanalysis over France with Safran-Isba-Modcou hydrometeorological suite. In: *Hydrological Earth System Sciences*, **14**. European Geosciences Union, pp. 459–478. <https://doi.org/10.5194/hess-14-459-2010>.
- Vicente-Serrano, S.M., López-Moreno, J.I., 2005. Hydrological response to a different time scales of climatological drought: an evaluation of the Standardized Precipitation Index in a mountainous Mediterranean basin. In: *Hydrological and Earth System Science*, **9**. European Geosciences Union, pp. 523–533. <https://doi.org/10.5194/hess-9-523-2005>.
- Wilhite, D.A., Svoboda, M.D., Hayes, M.J., 2007. Understanding the complex impacts of drought: a key to enhancing drought mitigation and preparedness. *Water Resour. Manag.* **21**, 763–774.
- Yue, S., Pilon, P., Phinney, B., Cavadias, G., 2002b. The influence of autocorrelation on the ability to detect trend in hydrological series. *Hydrol. Process.* **16**, 1807–1829.
- Yue, S., Pilon, P., Cavadias, G., 2002a. Power of the Mann-Kendall and Spearman’s rho tests for detecting monotonic trends in hydrological series. *J. Hydrol.* **259**, 254–271.